J|A|C|S ARTICLES

Published on Web 05/17/2010

Variation in Quadrupole Couplings of α Deuterons in Ubiquitin Suggests the Presence of $C^{\alpha}-H^{\alpha}\cdots O{=}C$ Hydrogen Bonds

Devon Sheppard,[†] Da-Wei Li,[‡] Raquel Godoy-Ruiz,[†] Rafael Brüschweiler,[‡] and Vitali Tugarinov*[,†]

Department of Chemistry and Biochemistry, University of Maryland, College Park, Maryland 20742, and Chemical Sciences Laboratory, Department of Chemistry and Biochemistry, and National High Magnetic Field Laboratory, Florida State University, Tallahassee, Florida 32306

Received February 27, 2010; E-mail: vitali@umd.edu

Abstract: Nuclear quadrupolar couplings are sensitive probes of hydrogen bonding. Experimental quadrupolar coupling constants of α deuterons (D^{α} QCC) are reported for the residues of human ubiquitin that do not experience large-amplitude internal dynamics on the pico- to nanosecond time scale. Two different methods for D^{α} QCC estimation are employed: (i) direct estimation of D^{α} QCC values from R_1 and R_2 ^2H D^{α} rates using the dynamics parameters ($S^2_{C\alpha-H\alpha}$) derived from 1 μs molecular dynamics simulations as well as from $^{13}C^{\alpha}$ relaxation measurements and (ii) indirect measurements via scalar relaxation of the second kind that affects $^{13}C^{\alpha}$ relaxation rates in $^{13}C^{\alpha}-D^{\alpha}$ spin systems. A relatively large variability of D^{α} QCC values is produced by both methods. The average value of 170.6 ± 3 kHz is derived from the combined data set, with D^{α} QCC values ranging from 159.2 to 177.2 kHz. The set of lowest quadrupolar couplings in all data sets corresponds to the residues that are likely to form weak $C^{\alpha}-H^{\alpha}\cdots O{=}C$ hydrogen bonds as predicted from the analysis of short $H^{\alpha}\cdots O$ distances in three-dimensional structures of ubiquitin. These D^{α} nuclei show up to 10 kHz reduction in their QCC values, which is in agreement with earlier solid-state NMR measurements in α deuterons of glycine. A statistically significant correlation is observed between the QCC values of α-deuterons and the inverse cube of $C^{\alpha}-H^{\alpha}\cdots O{=}C$ distances in ubiquitin.

Introduction

The popularity of deuterium nuclei as probes of molecular dynamics in proteins stems from the fact that ^2H relaxation is completely dominated by the strong and local quadrupolar mechanism.[1] Typically, the knowledge of only a single parameter, the ^2H quadrupole coupling constant (QCC), is needed for the interpretation of ^2H relaxation data in terms of order parameters of bond vector motions. On the other hand, if the dynamics parameters of bond vector motions are known with sufficient accuracy, for example, from molecular dynamics simulations or independent relaxation measurements of another nucleus in the same bond vector,[2] the ^2H QCC values can be evaluated.

^2H QCC values have been long recognized as sensitive probes of hydrogen bonding.[2−6] Typically, lower QCC values are obtained for deuterons involved in hydrogen bonds because of the higher symmetry of the electronic environment around the nucleus created by the overlap of electronic wave functions of hydrogen bond donor and acceptor groups. For example, amide deuterium QCC values vary in the range between approximately 200 and 240 kHz in proteins depending on the strength of the involved hydrogen bond.[2,5] Anticorrelations between ^2H QCC values and hydrogen bond strengths of the form $a + b/r^3$, where r is the hydrogen bond length and a and b are coefficients that depend on the type of hydrogen bond donor and acceptor, have been obtained in small molecules as well as in proteins.[2−5]

The NMR methodology for the measurement of ^2H relaxation rates in proteins has undergone intensive development in the past decade.[7−9] Previously, ^2H relaxation measurements in proteins were confined to side chain deuterons: methyl groups of the $^{13}CH_2D$[7,8,10,11] or $^{13}CHD_2$[12] variety, side chain ^{13}CHD groups,[13] or ^{15}NHD moieties of asparagine and glutamine side chains.[14] Recently, NMR methods have been developed that

[†] University of Maryland.
[‡] Florida State University.

(1) Abragam, A. *Principles of Nuclear Magnetism*; Clarendon Press: Oxford, U.K., 1961.
(2) Sheppard, D.; Tugarinov, V. *J. Magn. Reson.* **2010**, *203*, 316–322.
(3) Soda, G.; Chiba, T. *J. Chem. Phys.* **1969**, *50*, 439–446.
(4) Hunt, M. J.; Mackay, A. L. *J. Magn. Reson.* **1976**, *22*, 295–301.
(5) LiWang, A. C.; Bax, A. *J. Magn. Reson.* **1997**, *127*, 54–64.
(6) Muller, C.; Schajor, W.; Zimmermann, H.; Haeberlen, U. *J. Magn. Reson.* **1984**, *56*, 235–346.
(7) Muhandiram, D. R.; Yamazaki, T.; Sykes, B. D.; Kay, L. E. *J. Am. Chem. Soc.* **1995**, *117*, 11536–11544.
(8) Millet, O.; Muhandiram, D. R.; Skrynnikov, N. R.; Kay, L. E. *J. Am. Chem. Soc.* **2002**, *124*, 6439–6448.
(9) Skrynnikov, N. R.; Millet, O.; Kay, L. E. *J. Am. Chem. Soc.* **2002**, *124*, 6449–6460.
(10) Millet, O.; Mittermaier, A.; Baker, D.; Kay, L. E. *J. Mol. Biol.* **2003**, *329*, 551–563.
(11) Tugarinov, V.; Ollerenshaw, J. E.; Kay, L. E. *J. Am. Chem. Soc.* **2005**, *127*, 8214–8225.
(12) Tugarinov, V.; Kay, L. E. *J. Am. Chem. Soc.* **2006**, *128*, 12484–12489.
(13) Yang, D.; Mittermaier, A.; Mok, Y. K.; Kay, L. E. *J. Mol. Biol.* **1998**, *276*, 939–954.
(14) Pervushin, K.; Wider, G.; Wüthrich, K. *J. Am. Chem. Soc.* **1997**, *119*, 3842–3843.

extend the utility of deuterium as a probe of motions to α positions (D^α) in the backbones of [U-^{15}N,^{13}C,^{2}H]-labeled proteins.[15] The D^α ^{2}H-derived measures of backbone order have been shown to be in good agreement with 1 μs molecular dynamics (MD) simulations.[15] In this earlier study, a uniform QCC value has been assumed for all α sites of the polypeptide chain. On the basis of the measurement of ratios of quadrupolar splittings and residual dipolar couplings in an oriented protein,[16] a D^α QCC estimate of 174 kHz has been obtained.[15] However, the best agreement between the amplitudes of $C^\alpha-H^\alpha$ bond vector motions (squared order parameters, $S^2_{C^\alpha-H^\alpha}$) derived from 1 μs MD simulations and ^{2}H measurements was obtained when a reduced D^α QCC value of 171 kHz was used.[15]

To resolve this discrepancy and to assess the range of variability of D^α QCC values in proteins, D^α QCC values are determined in ubiquitin (27 °C) for the residues that do not undergo large-amplitude dynamics on the pico- to nanosecond time scale using two different methods: (i) direct estimation of D^α QCC from R_1 and R_2 ^{2}H D^α rates using the dynamics parameters ($S^2_{C^\alpha-H^\alpha}$) derived from 1 μs molecular dynamics (MD) simulations as well as from $^{13}C^\alpha$ relaxation measurements and (ii) indirect measurements via scalar relaxation of the second kind that affects the decay of $^{13}C^\alpha$ magnetization in $^{13}C^\alpha-D^\alpha$ spin systems, using the methodology derived from that developed earlier for QCC measurements in amide deuterons.[5] A larger than expected variability of the derived D^α QCC values is obtained with both methods. The average D^α QCC value of 170.6 ± 3 kHz is derived from the combined data set, with individual D^α QCC values ranging from 162 to 177 kHz. The set of lowest quadrupolar couplings in all data sets corresponds to the residues that are likely to form weak $C^\alpha-H^\alpha\cdots O{=}C$ hydrogen bonds[17−19] as suggested by their short (<2.5 Å) $H^\alpha\cdots O{=}C$ distances in three-dimensional structures of ubiquitin. The variability of D^α QCC values in ubiquitin confirms that hydrogen bonds are not confined to amide and hydroxyl moieties in protein structures providing an additional structural motif of enthalpic stabilization. The first direct observation of $C^\alpha-H^\alpha\cdots O{=}C$ hydrogen bonds by solution NMR was reported by Grzesiek and co-workers via the measurement of inter-residual (trans-hydrogen bond) $^{h3}J_{C^\alpha C'}$ scalar couplings (∼0.3 Hz) in protein G.[19] This work represents the first indirect detection of these weak interactions by ^{2}H solution NMR techniques.

Materials and Methods

Protein Samples. Three isotopically labeled samples of wild-type human ubiquitin have been used in this work: (i) fractionally ^{13}C-enriched sample obtained using [2-$^{13}C_1$]-glucose as the principal carbon source (termed the [2-$^{13}C_1$]-glucose-derived sample in the text), (ii) [U-^{15}N,^{13}C,^{2}H]-ubiquitin used previously for ^{2}H D^α relaxation measurements,[15] and (iii) [U-^{15}N,^{13}C]-ubiquitin used for $^1J_{C^\alpha H^\alpha}$ scalar coupling measurements. The patterns of ^{13}C enrichment obtained for [2-$^{13}C_1$]-glucose-derived protein samples have been described in detail previously[20] and are briefly discussed in Results and Discussion in the context of $^{13}C^\alpha$ relaxation measurements. The [2-$^{13}C_1$]-glucose-derived and [U-^{15}N,^{13}C,^{2}H]-labeled NMR samples were 3 mM in protein concentration and were dissolved in a 20 mM 90% H_2O/10% D_2O sodium phosphate buffer (pH 6.8) containing 0.03% NaN_3. The [U-^{15}N,^{13}C]-ubiquitin was 2.0 mM in protein concentration and was dissolved in a 99.9% D_2O sodium phosphate buffer (pD 6.8, uncorrected).

NMR Spectroscopy. All NMR experiments were performed on a 600 MHz Bruker Avance III spectrometer equipped with a room-temperature triple-resonance *z*-gradient probe operating at 27 °C. $^{13}C^\alpha$ $R_{1\rho}$, R_1, and $\{^1H_\alpha\}-^{13}C_\alpha$ NOE experiments were conducted with the [2-$^{13}C_1$]-glucose-derived sample of ubiquitin using a straightforward adaptation of the gradient sensitivity-enhanced pulse schemes commonly used for ^{15}N relaxation rate measurements. $^{13}C^\alpha$ $R_{1\rho}$ and R_1 rates were recorded using parametrically varied delays of 2, 10, 20, 30, 40, 50, and 60 ms and 20, 100, 200, 300, 400, 500, and 600 ms, respectively. The $^{13}C^\alpha$ $R_{1\rho}$ experiment employed a spin-lock strength of 2 kHz, with the ^{13}C carrier positioned at 58 ppm. $R_{1\rho}$ values were subsequently corrected for off-resonance effects to yield $^{13}C^\alpha$ R_2 rates. $\{^1H^\alpha\}-^{13}C^\alpha$ NOE experiments were performed using a total relaxation delay of 6 s with a 4 s long presaturation period. Each of the $^{13}C^\alpha$ $R_{1\rho}$ and R_1 experiments was conducted for 4 h, while each of the $\{^1H^\alpha\}-^{13}C^\alpha$ NOE data sets was acquired in 6 h.

$^{13}C^\alpha$ CPMG[21,22] measurements were performed on [U-^{15}N,^{13}C,^{2}H]-ubiquitin using the pulse scheme of Figure 1. The scheme derives from a gradient sensitivity-enhanced HN(COCA)[23] experiment. The relaxation of $^{13}C^\alpha$ nuclei due to scalar coupling to α deuterons is quantified via the performance of two experiments: (i) with ^{2}H decoupling (shown with the shaded dashed rectangle in Figure 1) and (ii) without ^{2}H decoupling during the CPMG[21,22] delay *T*. The ratios of cross-peak intensities obtained in the $^{13}C^\alpha$ CPMG measurements without ^{2}H decoupling (I_a) and with ^{2}H decoupling (I_b), I_a/I_b, are interpreted as described in Results and Discussion. All narrow (wide) rectangular pulses were applied with flip angles of 90° (180°) along the *x*-axis unless indicated otherwise. The ^{1}H (^{2}H; ^{15}N) carriers are positioned at 4.7 ppm (4.5 ppm; 119 ppm). The ^{13}C carrier is placed at 176 ppm, switched to 58 ppm before the first 90° $^{13}C^\alpha$ pulse (after gradient g5), and switched back to 176 ppm after the last 90° $^{13}C^\alpha$ pulse (following gradient g7). ^{15}N WALTZ-16[24] decoupling during acquisition was achieved using a 1.25 kHz field. ^{2}H WALTZ-16[24] decoupling during the 2ε period used a 0.9 kHz field, while a continuous-wave (CW) ^{2}H decoupling with a field strength of 1.3 kHz was used during the CPMG train (delay *T*). No increases in the extracted QCC values were observed when stronger (1.7 kHz) CW or WALTZ-16 ^{2}H decoupling was used during the CPMG period. SEDUCE[25,26] $^{13}C^\alpha$ decoupling was implemented with 300 μs seduce-shaped pulses applied at $^{13}C^\alpha$ frequency by phase modulation of the carrier.[27,28] ^{1}H WALTZ-16 decoupling was applied with a 7 kHz field. All ^{1}H and ^{15}N pulses were applied with the maximum possible power, while 90° (180°) ^{13}C rectangular pulses were applied with a field strength of $\Delta/\sqrt{15}$ ($\Delta/\sqrt{3}$), where Δ is the difference in hertz between the $^{13}C^\alpha$ and ^{13}CO chemical shifts.[29] Vertical arrows at the beginning and end of the $2\tau_c$ periods indicate the position of the ^{13}CO Bloch−Siegert shift compensation pulses.[29] $^{13}C^\alpha$-shaped pulses in the middle of the *T* periods are 150 μs (600 MHz) 180° Q3 Gaussian cascade pulses[30] centered at 20 ppm by phase modulation of the carrier

(15) Sheppard, D.; Li, D. W.; Brüschweiler, R.; Tugarinov, V. *J. Am. Chem. Soc.* **2009**, *131*, 15853–15865.
(16) Mittermaier, A.; Kay, L. E. *J. Am. Chem. Soc.* **1999**, *121*, 10608–10613.
(17) Sutor, D. J. *Nature* **1962**, *195*, 68–69.
(18) Taylor, R.; Kennard, O. *J. Am. Chem. Soc.* **1982**, *104*, 5063–5070.
(19) Cordier, F.; Barfield, M.; Grzesiek, S. *J. Am. Chem. Soc.* **2003**, *125*, 15750–15751.
(20) Lundström, P.; Teilum, K.; Carstensen, T.; Bezsonova, I.; Wiesner, S.; Hansen, D. F.; Religa, T. L.; Akke, M.; Kay, L. E. *J. Biomol. NMR* **2007**, *38*, 199–212.
(21) Meiboom, S.; Gill, D. *Rev. Sci. Instrum.* **1958**, *29*, 688.
(22) Carr, H. Y.; Purcell, E. M. *Phys. Rev.* **1954**, *94*, 630–638.
(23) Bax, A.; Ikura, M. *J. Biomol. NMR* **1991**, *1*, 99–104.
(24) Shaka, A. J.; Keeler, J.; Frenkiel, T.; Freeman, R. *J. Magn. Reson.* **1983**, *52*, 335–338.
(25) McCoy, M. A.; Mueller, L. *J. Magn. Reson.* **1992**, *98*, 674–679.
(26) McCoy, M. A.; Mueller, L. *J. Am. Chem. Soc.* **1992**, *114*, 2108–2112.
(27) Patt, S. L. *J. Magn. Reson.* **1992**, *96*, 94–102.
(28) Boyd, J.; Soffe, N. *J. Magn. Reson.* **1989**, *85*, 406–413.
(29) Kay, L. E.; Ikura, M.; Tschudin, R.; Bax, A. *J. Magn. Reson.* **1990**, *89*, 496–514.
(30) Emsley, L.; Bodenhausen, G. *Chem. Phys. Lett.* **1987**, *165*, 469–476.

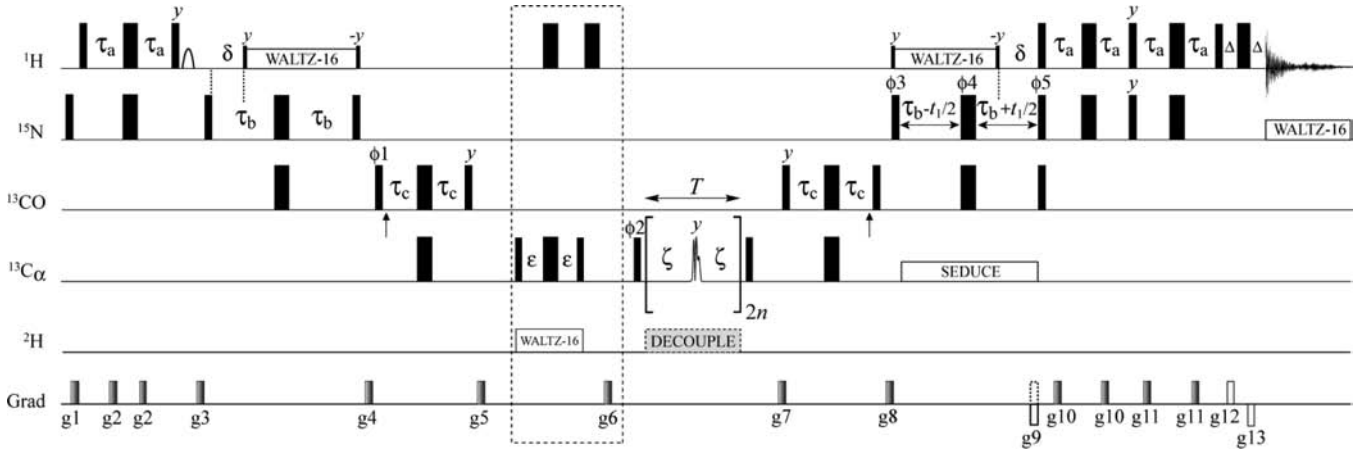

Figure 1. HN(COCA)-based $^{13}C^{\alpha}$ CPMG pulse scheme employed for the measurement of D^{α} QCC values via scalar relaxation of the second kind. The element enclosed in the dashed rectangle is designed to eliminate signals from (residually) protonated $^{13}C^{\alpha}$ positions (see the text). The experimental details are described in Materials and Methods.

that cover the range of all ^{13}C aliphatic chemical shifts without disturbing $^{13}C'$ nuclei (refocusing bandwidth of 7.9 kHz). The ^{1}H pulse preceding gradient g3 and shown with an arc is implemented as a water-selective 1.5 ms rectangular pulse. Delays are as follows: $\tau_a = 2.7$ ms, $\tau_b = 12.5$ ms, $\tau_c = 4.5$ ms, $\delta = 5.4$ ms, $\varepsilon = 1.75$ ms, $\zeta = 3.5$ ms (a 7 ms delay between CPMG pulses), and $\Delta = 0.4$ ms. The CPMG delay T is enclosed in rectangular parentheses. Total CPMG durations T equal to integer multiples of $1/^1J_{CC}$ have been used: 28, 56, and 84 ms corresponding to 4, 8, and 12 CPMG cycles, respectively [$n = 2$, 4, or 6 (Figure 1)]. The phase cycle is as follows: $\phi1 = x,-x$; $\phi2 = 2(x),2(-x)$; $\phi3 = 4(x),4(-x)$; $\phi4 = 8(x),8(-x)$; $\phi5 = x$; rec. $= x,-x,-x,x,-x,x,x,-x$. Quadrature detection in t_1 is achieved via the Rance−Kay scheme:[31−33] for each t_1 value, a pair of spectra is recorded with ($\phi5 = x$; g9) and ($\phi5 = -x$; −g9) and manipulated postacquisition. Phase $\phi3$ is inverted for each t_1 point.[34] Durations and strengths of pulsed field gradients in units of milliseconds and Gauss per centimeter, respectively, are as follows: g1 = (1;15); g2 = (0.25;5); g3 = (1.2;12); g4 = (0.5;8); g5 = (0.6;10); g6 = (1.0;12); g7 = (0.7;15); g8 = (0.6;10); g9 = (1.25;20); g10 = (0.25;8); g11 = (0.3;5); g12 = (0.0625;20); g13 = (0.0625;−20). Each of the $^{13}C^{\alpha}$ CPMG experiments (with and without ^{2}H decoupling) was conducted in 22 h.

$^1J_{C^{\alpha}H^{\alpha}}$ scalar couplings have been measured on the [U-^{15}N,^{13}C]-ubiquitin using the J modulation scheme of Tjandra and Bax.[35] The obtained $^1J_{C^{\alpha}H^{\alpha}}$ values are in excellent agreement with those reported for ubiquitin previously.[35] For analysis of the $^{13}C^{\alpha}$ CPMG measurements (performed on $^{13}C^{\alpha}-D^{\alpha}$ spin pairs), the $^1J_{C^{\alpha}H^{\alpha}}$ values have been scaled by the ratio γ_D/γ_H, where γ_i is the gyromagnetic ratio of nucleus i.

Data Analysis. All NMR spectra were processed using the NMRPipe/NMRDraw suite of programs and associated software.[36] $^{13}C^{\alpha}$ relaxation rates were obtained by fitting peak intensities to a single-exponential function of the form $I = I_0 \exp(-RT)$, where I is the measured intensity and R is the relaxation rate. Errors in peak intensities have been estimated from duplicate measurements or from the noise-floor level of the spectra, whichever was the highest, and subsequently propagated to the errors in the extracted rates using Monte Carlo analysis.[37] $^{13}C^{\alpha}$ R_1, R_2, and $\{^1H^{\alpha}\}-^{13}C^{\alpha}$ NOE data have been subjected to conventional model-free analysis[38,39] using theoretical expressions for dipolar and chemical shift anisotropy (CSA) relaxation rates in two-spin X−H ($^{13}C^{\alpha}-^1H^{\alpha}$) systems.[40] The following form of the spectral density function for an axially symmetric orientational molecular diffusion tensor[38,39,41] was used in all calculations:

$$J(\omega) = S^2\left[\frac{A_1\tau_1}{1+(\omega\tau_1)^2} + \frac{A_2\tau_2}{1+(\omega\tau_2)^2} + \frac{A_3\tau_3}{1+(\omega\tau_3)^2}\right] + (1-S^2)\frac{\tau'}{1+(\omega\tau')^2} \quad (1)$$

where S^2 is the generalized order parameter squared describing the fluctuations of $C^{\alpha}-H^{\alpha}$ bond vectors ($S^2_{C^{\alpha}-H^{\alpha}}$), $A_1 = (3/4)\sin^4(\beta)$, $A_2 = 3\sin^2(\beta)\cos^2(\beta)$, $A_3 = [(3/2)\cos^2(\beta) - 0.5]^2$, $\tau_1 = (4D_{||} + 2D_{\perp})^{-1}$, $\tau_2 = (D_{||} + 5D_{\perp})^{-1}$, $\tau_3 = (6D_{\perp})^{-1}$, $D_{||}$ and $D_{\perp}$ are the parallel and perpendicular components of the molecular diffusion tensor, respectively, β is the angle between the $C^{\alpha}-H^{\alpha}$ bond vector and the unique diffusion axis, and $1/\tau' = 1/\tau_f + 1/\tau_{c,eff}$, where the effective correlation time of overall rotation $\tau_{c,eff} = (2D_{||} + 4D_{\perp})^{-1}$ and τ_f is the correlation time of fast local motions. Direction cosines for $C^{\alpha}-H^{\alpha}$ bond vectors of human ubiquitin have been obtained from the protonated crystal structure of ubiquitin [Protein Data Bank (PDB) entry 1ubq].[42]

We have accounted for contributions to $^{13}C^{\alpha}$ R_1 and R_2 rates due to dipolar interactions with external protons by calculating a cumulative effective distance from each $^{13}C^{\alpha}$ position to all external protons in the molecule (including protonated amides). A $C^{\alpha}-H^{\alpha}$ distance of 1.09 Å was used for all calculations.[43,44] The $^{13}C^{\alpha}$ CSA is small,[45] barely affecting the extracted $^{13}C^{\alpha}$ dynamics parameters.[40,46,47] Residue-specific CSA values in ubiquitin ($^{13}C^{\alpha}$ CSA tensor assumed to be axially symmetric) were taken from ref 45.

(31) Palmer, A. G.; Cavanagh, J.; Wright, P. E.; Rance, M. *J. Magn. Reson.* **1991**, *93*, 151–170.
(32) Kay, L. E.; Keifer, P.; Saarinen, T. *J. Am. Chem. Soc.* **1992**, *114*, 10663–10665.
(33) Schleucher, J.; Sattler, M.; Griesinger, C. *Angew. Chem., Int. Ed.* **1993**, *32*, 1489–1491.
(34) Marion, D.; Ikura, M.; Tschudin, R.; Bax, A. *J. Magn. Reson.* **1989**, *85*, 393–399.
(35) Tjandra, N.; Bax, A. *J. Magn. Reson.* **1997**, *124*, 512–515.
(36) Delaglio, F.; Grzesiek, S.; Vuister, G. W.; Zhu, G.; Pfeifer, J.; Bax, A. *J. Biomol. NMR* **1995**, *6*, 277–293.
(37) Kamith, U.; Shriver, J. W. *J. Biol. Chem.* **1989**, *264*, 5586–5592.
(38) Lipari, G.; Szabo, A. *J. Am. Chem. Soc.* **1982**, *104*, 4559–4570.
(39) Lipari, G.; Szabo, A. *J. Am. Chem. Soc.* **1982**, *104*, 4546–4559.
(40) Palmer, A. G. I.; Hochstrasser, R. A.; Millar, D. P.; Rance, M.; Wright, P. E. *J. Am. Chem. Soc.* **1993**, *115*, 6333–6345.
(41) Woessner, D. E. *J. Chem. Phys.* **1962**, *37*, 647–654.
(42) Vijay-Kumar, S.; Bugg, C. E.; Cook, W. J. *J. Mol. Biol.* **1987**, *194*, 531–544.
(43) Jeffrey, G. *Accurate molecular structures, their determination and importance*; Oxford University Press: Oxford, U.K., 1992.
(44) Ottiger, M.; Bax, A. *J. Am. Chem. Soc.* **1998**, *120*, 12334–12341.
(45) Tjandra, N.; Bax, A. *J. Am. Chem. Soc.* **1997**, *119*, 9576–9577.

The errors in the ratios of cross-peak intensities obtained in the $^{13}C^{\alpha}$ CPMG experiments (I_a/I_b) were estimated from duplicate measurements. $^{13}C^{\alpha}$ CPMG experiments were repeated three times, and the best-fit D^{α} QCC values were examined for reproducibility and subsequently averaged. The fitting procedure was implemented as described in Results and Discussion using numerical integration of eq S3 (see the Supporting Information) that includes the effects of $^{13}C^{\alpha}-D^{\alpha}$ dipolar/D^{α} quadrupolar cross-correlated relaxation.[48] The quality of the fits for a total of three CPMG durations (T) was estimated by the goodness-of-fit (χ^2) test with two degrees of freedom.[49] For the sake of consistency with the set of previously obtained $R^Q(D_+)$ and $R^Q(D_z)$ rates of D^{α} deuterons in ubiquitin at 27 °C,[15] all D^{α} QCC calculations in this work were performed using the parameters of global diffusion of ubiquitin determined from D^{α} ^2H relaxation:[15] $\tau_{c,eff} = 3.94$ ns, $D_{\parallel}/D_{\perp} = 1.22$, $\theta = 8°$, and $\phi = -8°$, where the polar angles θ and ϕ, which determine the orientation of the unique axis of the global diffusion tensor, are specified in the inertial coordinate frame.

Molecular Dynamics Simulations. A 1 μs all-atom MD trajectory of ubiquitin in explicit water was performed using Amber9[50,51] with the Amber99SB force field[51] as described in detail previously.[15] The values of $S^2_{C^{\alpha}-H^{\alpha}}$ were extracted using the iRED method[52] averaged over time windows of 5 ns, on the order of the experimental global tumbling correlation time of ubiquitin. The MD simulation was conducted on two dual-core 2.2 GHz AMD Opteron machines with a production rate of 2 ns per day.

Results and Discussion

Determination of quadrupolar couplings by solution NMR methods requires accurate knowledge of the parameters of the spectral density function: those related to the global rotational diffusion as well as the fluctuations of individual bond vectors on a faster time scale (local dynamics).[5] While the former can be established with sufficient accuracy, the latter may be dependent on the model used for the interpretation of spin relaxation rates. That is why our analysis is restricted to the residues where local dynamics can be adequately described by the simplest form of the spectral density, i.e., the protein sites that are relatively "rigid" and do not undergo large-amplitude motions. We first describe two different methods for D^{α} QCC estimation: (i) direct evaluation from R_1 and R_2 ^2H D^{α} rates[15] assuming the order parameters of $C^{\alpha}-D^{\alpha}$ bond vector motions ($S^2_{C^{\alpha}-D^{\alpha}}$) evaluated independently[2] (derived from MD simulations and $^{13}C^{\alpha}$ relaxation rates) and (ii) the indirect approach of LiWang and Bax[5] adapted to $^{13}C^{\alpha}-D^{\alpha}$ spin systems that involves indirect QCC measurements via scalar relaxation affecting the decay of $^{13}C^{\alpha}$ nuclei. Besides $S^2_{C^{\alpha}-D^{\alpha}}$, this second technique[5] requires accurate knowledge of one-bond scalar couplings $^1J_{C^{\alpha}-D^{\alpha}}$ and is, in general, more experimentally demanding. However, it provides an important experimental verification of the directly calculated QCC values.

Direct Determination of D^{α} QCC Values from ^2H D^{α} $R^Q(D_+)$ and $R^Q(D_z)$ Relaxation Rates. The relaxation rates of ^2H transverse and longitudinal magnetization are given by[1]

$$R^Q(D_+) = R_2^Q = \frac{\pi^2}{20}(QCC)^2[9J(0) + 15J(\omega_D) + 6J(2\omega_D)] \quad (2)$$

$$R^Q(D_z) = R_1^Q = \frac{3\pi^2}{10}(QCC)^2[J(\omega_D) + 4J(2\omega_D)] \quad (3)$$

where QCC $= (e^2qQ/h)$ is the quadrupolar coupling constant in hertz, $J(\omega_D)$ is the spectral density function of eq 1 evaluated at frequency ω_D, and $S^2 \equiv S^2_{C^{\alpha}-D^{\alpha}}$. The asymmetry of the ^2H electric field gradient tensor in aliphatic deuterons is typically <0.04[53,54] and can be safely neglected. To a good approximation, the principal axis of the axially symmetric electric field gradient tensor is parallel to the direction of the C−D bond.[6] Then, the anisotropy of the electric field gradient tensor represented by the value of QCC is the main characteristic of the quadrupolar tensor that enters into eqs 2 and 3. Clearly, provided that global and local dynamics parameters describing the spectral density function $J(\omega)$ (eq 1) are known with sufficient accuracy, D^{α} QCC can be evaluated from $R^Q(D_+)$ and $R^Q(D_z)$ rates. The parameters of global molecular reorientation can be obtained from ^{15}N, ^2H,[15,55] or $^{13}C^{\alpha}$ [56] relaxation studies. On the other hand, the dynamics of the majority of $C^{\alpha}-D^{\alpha}$ bond vectors in ubiquitin can be adequately described using a single-parameter ($S^2_{C^{\alpha}-D^{\alpha}}$) spectral density (with τ' set to zero in eq 1).[15] In our earlier study of D^{α} ^2H relaxation, $S^2_{C^{\alpha}-D^{\alpha}}$ values have been derived under the assumption of uniform D^{α} QCCs of 174 or 171 kHz.[15] Evidently, for the extraction of D^{α} QCC values, estimates of order parameters of the $C^{\alpha}-D^{\alpha}$ bond vectors should be used that do not depend on QCC. In principle, such estimates are provided by MD simulations. In practice, however, the MD-derived order parameters depend on the quality of the molecular mechanics force field used as well as the simulation protocol and analysis methods employed.[57−60] Therefore, we have chosen to validate the adequacy of MD-derived S^2 values in ubiquitin with $^{13}C^{\alpha}$ relaxation measurements.

The main assumption involved in this analysis is that the amplitudes of motions of $^{13}C^{\alpha}-^1H^{\alpha}$ spin pairs as monitored by $^{13}C^{\alpha}$ relaxation in protonated protein samples are the same as those of $^{13}C^{\alpha}-D^{\alpha}$ pairs. Because the mass of the deuteron is double that of the proton, the amplitudes of local motions (S^2) may be affected by the ^1H-to-^2H substitution due to zero-point vibrational effects and a noticeable contribution of librational motions to S^2 in proteins.[61,62] Nevertheless, here we assume that these changes are small. Indeed, the directly measured ^{15}N rates in $^{15}N-D$ spin pairs of protein G have been found in good agreement with theoretical predictions based on the micro-dynamic parameters (S^2_{NH} and τ_f) obtained from ^{15}N data in

(46) Engelke, J.; Rüterjans, H. *J. Biomol. NMR* **1995**, *5*, 173–182.
(47) Engelke, J.; Rüterjans, H. In *Biological Magnetic Resonance: Structure Computation and Dynamics in Protein NMR*; Krishna, N. R., Berliner, L. J., Eds.; Kluwer Academic Publishers: New York, 1999; Vol. 17.
(48) Grzesiek, S.; Bax, A. *J. Am. Chem. Soc.* **1994**, *116*, 10196–10201.
(49) Bevington, P. R.; Robinson, D. K. *Data Reduction and Error Analysis for the Physical Sciences*; WCB/McGraw-Hill: New York, 1992.
(50) Case, D. A.; Cheatham, T. E.; Darden, T.; Gohlke, H.; Luo, R.; Merz, K. M.; Onufriev, A.; Simmerling, C.; Wang, B.; Woods, R. J. *J. Comput. Chem.* **2005**, *26*, 1668–1688.
(51) Hornak, V.; Abel, R.; Okur, A.; Strockbine, B.; Roitberg, A.; Simmerling, C. *Proteins* **2006**, *65*, 712–725.
(52) Prompers, J. J.; Brüschweiler, R. *J. Am. Chem. Soc.* **2002**, *124*, 4522–4534.
(53) Wooten, J. B.; Savitsky, G. B.; Jacobus, J.; Beyerlein, A. L.; Emsley, J. W. *J. Chem. Phys.* **1979**, *70*, 438–442.
(54) Schramm, S.; Oldfield, E. *Biochemistry* **1983**, *22*, 2908–2913.
(55) Tjandra, N.; Feller, S. E.; Pastor, R. W.; Bax, A. *J. Am. Chem. Soc.* **1995**, *117*, 12562–12566.
(56) Lee, L. K.; Rance, M.; Chazin, W. J.; Palmer, A. G. *J. Biomol. NMR* **1997**, *9*, 287–298.
(57) Showalter, S. A.; Brüschweiler, R. *J. Chem. Theory Comput.* **2007**, *3*, 961–975.
(58) Trbovic, N.; Kim, B.; Friesner, R. A.; Palmer, A. G. I. *Proteins* **2008**, *71*, 684–694.
(59) Koller, A. N.; Schwalbe, H.; Gohlke, H. *Biophys. J.* **2008**, *95*, L04–L06.
(60) Bui, J. M.; Gsponer, J.; Vendruscolo, M.; Dobson, C. M. *Biophys. J.* **2009**, *97*, 2513–2520.
(61) Brüschweiler, R. *J. Am. Chem. Soc.* **1992**, *114*, 5341–5344.
(62) Henry, E. R.; Szabo, A. *J. Chem. Phys.* **1985**, *82*, 4753–4761.

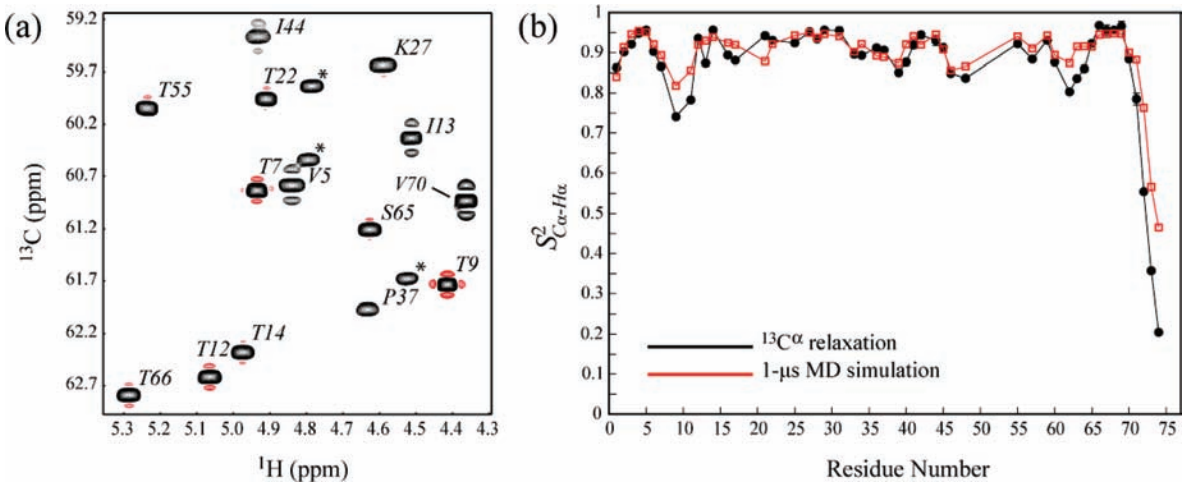

Figure 2. (a) Region of the $^{1}H^{\alpha}-^{13}C^{\alpha}$ correlation map of [2-$^{13}C_1$]-glucose-derived ubiquitin (27 °C, 600 MHz) acquired as the first measurement point of the $^{13}C^{\alpha}$ $R_{1\rho}$ experiment (10 ms relaxation delay). Cross-peaks of valines and isoleucines have the characteristic triplet structure arising from the superposition of ~25% $^{13}C^{\alpha}-^{13}C^{\beta}$-enriched doublets and ~25% $^{13}C^{\alpha}-^{12}C^{\beta}$-enriched singlets.[20] The peaks marked with asterisks arise from $^{1}H^{\beta}-^{13}C^{\beta}$ correlations of threonines that are residually $^{13}C^{\beta}$-enriched. Note that whenever Thr C^{β} positions are ^{13}C-labeled, Thr C^{α} and $C^{\gamma 2}$ positions remain at natural abundance so that $^{13}C^{\alpha}-^{13}C^{\beta}$ and $^{13}C^{\beta}-^{13}C^{\gamma 2}$ spin pairs are not observed. (b) $C^{\alpha}-H^{\alpha}$ bond vector order parameters ($S^2_{C\alpha-H\alpha}$) in ubiquitin (27 °C) obtained from $^{13}C^{\alpha}$ relaxation (black circles and lines) and from a 1 μs MD simulation (red squares and lines) plotted as a function of residue number.

$^{15}N-^{1}H$ amides.[63] Likewise, in our earlier D^{α} ^{2}H relaxation study, experimental $S^2_{C\alpha-D\alpha}$ order parameters were found to be in good agreement with $S^2_{C\alpha-H\alpha}$ derived from 1 μs MD simulations of protonated ubiquitin when the D^{α} QCC value of 171 kHz was assumed.[15]

Recent advances in isotope labeling technologies allow separation of individual $^{13}C^{\alpha}-^{1}H^{\alpha}$ spin pairs in protein molecules, so that $^{13}C^{\alpha}$ relaxation rates are not compounded by dipolar interactions with $^{13}C^{\beta}$ and ^{13}CO spins. One such labeling protocol introduced by Kay, Akke, and co-workers uses [2-$^{13}C_1$]-glucose as the primary carbon source in protein production media.[20] This leads to partial ^{13}C enrichment of all C^{α} positions in a protein except Leu, whereas $^{13}C^{\beta}$ and ^{13}CO positions remain at natural abundance. Thus, no $^{13}C^{\alpha}-^{13}C^{\beta}$ or $^{13}C^{\alpha}-^{13}$CO spin pairs are produced in the majority of residues (Ile and Val have some portion of $^{13}C^{\alpha}-^{13}C^{\beta}$ pairs), significantly simplifying analysis of $^{13}C^{\alpha}$ relaxation data.[20] This is especially true for analysis of $^{13}C^{\alpha}$ R_1 rates because cross-relaxation effects in $^{13}C^{\alpha}-^{13}C^{\beta}$ or $^{13}C^{\alpha}-^{13}$CO spin systems[64] are eliminated. Although the enrichment in ^{13}C is not complete (~45% or lower depending on the amino acid type), all residues except Leu appear with good sensitivity in $^{1}H-^{13}C$ correlations recorded on [2-$^{13}C_1$]-glucose-derived samples of small proteins. Figure 2a shows a region of the $^{1}H^{\alpha}-^{13}C^{\alpha}$ correlation map of the [2-$^{13}C_1$]-glucose-derived ubiquitin acquired as the first measurement point of the $^{13}C^{\alpha}$ $R_{1\rho}$ experiment. Notably, Ile and Val correlations appear as pseudotriplets arising from ~25% $^{13}C^{\alpha}-^{13}C^{\beta}$ labeling in these residues (Figure 1a). The Val and Ile residues where the central peak of the "triplet" corresponding to the isolated $^{13}C^{\alpha}$ position could not be sufficiently resolved from the outer correlations have been excluded from $^{13}C^{\alpha}$ relaxation analysis. This led to exclusion of two of four valines and four of seven isoleucines. Likewise, all glycine residues and seven of nine leucine residues (only ~5% $^{13}C^{\alpha}$ incorporation[20]) had to be excluded from analysis.

After exclusion of all residues likely to be involved in large-amplitude internal motions on a time scale τ' larger than a few hundred picoseconds ($\{^{1}H^{\alpha}\}-^{13}C^{\alpha}$ NOE > 1.25) or involved in conformational exchange, the R_1/R_2 analysis[55,65] of $^{13}C^{\alpha}$ relaxation rates of 44 residues in ubiquitin for which reliable data could be obtained yielded the following global diffusion tensor parameters for [2-$^{13}C_1$]-glucose-derived ubiquitin: $\tau_{c,eff} = 4.11 \pm 0.03$ ns, $D_{\parallel}/D_{\perp} = 1.19 \pm 0.02$, $\theta = 13 \pm 5°$, and $\phi = 16 \pm 10°$, where the polar angles θ and ϕ that determine the orientation of the unique axis of the global diffusion tensor are specified in the inertial coordinate frame. These values are in good agreement with the ^{15}N relaxation-derived parameters reported in our earlier study:[15] $\tau_{c,eff} = 4.16 \pm 0.01$ ns, $D_{\parallel}/D_{\perp} = 1.18 \pm 0.02$, $\theta = 6 \pm 2°$, and $\phi = -16 \pm 4°$. The extraction of global diffusion tensor parameters from $^{13}C^{\alpha}$ rates is somewhat less reliable than from ^{15}N data due to a smaller number of available probes and lower accuracy of $^{13}C^{\alpha}$ relaxation rates even when the latter are obtained from highly concentrated [2-$^{13}C_1$]-glucose-derived protein samples. Therefore, for the analysis of $^{13}C^{\alpha}$ rates in terms of $S^2_{C\alpha-H\alpha}$ and subsequent D^{α} QCC derivation, we have chosen to use the anisotropy and the orientation of the unique global diffusion axis as determined from ^{15}N data in conjunction with the $^{13}C^{\alpha}$ relaxation-derived value of $\tau_{c,eff}$ (4.11 ns).

Figure 2b compares $^{13}C^{\alpha}$ relaxation-derived $S^2_{C\alpha-H\alpha}$ values in ubiquitin (see Materials and Methods) with those obtained from analysis of MD trajectories for the same subset of 50 residues. Table S1 (Supporting Information) lists all $^{13}C^{\alpha}$ relaxation-derived and MD-derived $S^2_{C\alpha-H\alpha}$ in ubiquitin. Excellent agreement is found for the rigid portions of the structure (pairwise rmsd of only 0.023 between the two sets of $S^2_{C\alpha-H\alpha}$ values for the subset of 41 rigid residues; Pearson's $R = 0.92$). In flexible loops of the protein ($Thr^{9}-Lys^{11}$ and $Ile^{61}-Lys^{63}$) and the C-terminus ($Lys^{71}-Leu^{73}$), however, the experimental $S^2_{C\alpha-H\alpha}$ values tend to be systematically lower. This may arise either from the computational limitations mentioned above or from more complicated motional characteristics of the residues in the

(63) Vasos, P. R.; Hall, J. B.; Kummerle, R.; Fushman, D. *J. Biomol. NMR* **2006**, *36*, 27–36.
(64) Yamazaki, T.; Muhandiram, R.; Kay, L. E. *J. Am. Chem. Soc.* **1994**, *116*, 8266–8278.
(65) Kay, L. E.; Torchia, D. A.; Bax, A. *Biochemistry* **1989**, *28*, 8972–8979.

flexible regions, necessitating the invocation of an extended model-free spectral density function[66] for the interpretation of the experiment. Since in this work we concentrate on the residues with minimal contributions to $J(\omega)$ from large-amplitude dynamics, the level of agreement in Figure 2b achieved for the more rigid portions of the protein lends confidence in our in silico-derived $S^2_{C\alpha-H\alpha}$.

The D^α QCC values have been obtained from the simultaneous single-parameter best fit of the previously quantified $R^Q(D_+)$ and $R^Q(D_z)$ rates[15] (eqs 2 and 3) using (i) the MD-derived and (ii) $^{13}C^\alpha$-relaxation-derived $S^2_{C\alpha-H\alpha}$ for the rigid subset of residues in ubiquitin. Not surprisingly, similar distributions of QCC values have been obtained in both cases. D^α QCC values vary between 162.8 ± 1.4 (162.3 ± 1.4) kHz for Val[5] and 175.5 ± 0.8 (175.9 ± 1.2) kHz for Ser[57] in the MD-derived $S^2_{C\alpha-H\alpha}$ ($^{13}C^\alpha$ relaxation-derived $S^2_{C\alpha-H\alpha}$) sets. Of note, very similar results are obtained when D^α QCC is simply recalculated from the sum of $R^Q(D_+)$ and $R^Q(D_z)$ under the assumption of equal errors in $R^Q(D_+)$ and $R^Q(D_z)$, the pairwise rmsd of 2.2 kHz between the two sets of QCC values.

Scalar Relaxation-Based Estimation of D^α QCC Values in Ubiquitin. An alternative approach to the estimation of D^α QCC values relies upon scalar interactions in the $^{13}C^\alpha-D^\alpha$ spin systems, whereby the decay of the transverse $^{13}C^\alpha$ magnetization due to scalar coupling to fast-relaxing α-deuterons is monitored during a CPMG pulse train period.[5] Thus, D^α longitudinal relaxation rates are measured indirectly through their effect on $^{13}C^\alpha$ magnetization decay, and D^α QCC is estimated from longitudinal ^2H rates for the subset of residues with known dynamics parameters (S^2 and τ_f). Earlier, LiWang and Bax determined the QCC values of a subset of 35 amide deuterons in ubiquitin using indirect measurements of the effect of scalar relaxation of the second kind[1] on the ^{15}N relaxation rates in backbone ^{15}ND amides.[5] A conceptually similar but technically different approach was adopted by Boyd et al.[67] for QCC measurements in ^{15}NHD moieties of Asn and Gln side chains. Here, we closely follow the approach of LiWang and Bax[5] adapted for $^{13}C^\alpha-D^\alpha$ spin systems in proteins. Figure 1 shows the pulse scheme designed for the measurement of the effects of scalar relaxation of the second kind in $^{13}C^\alpha-D^\alpha$ spin pairs. In this 2D HN(COCA)[23]-derived experiment, the $^{13}C^\alpha$ 90° pulse applied with phase $\phi 2$ creates magnetization terms $4N_zC'_zC^\alpha_{tr}$, where tr denotes transverse magnetization and A_m denotes the spin operator for nucleus A ($m = x, y, z$). The transverse $^{13}C^\alpha$ magnetization then decays during CPMG delay T. For $\phi 2 = x$, in the Cartesian basis, the two outer lines ($|\!|+1\rangle\!\rangle_y$;$|\!|-1\rangle\!\rangle_y$) and the middle line ($|\!|0\rangle\!\rangle_y$) of the $^{13}C^\alpha-D^\alpha$ triplet can be expressed as

$$|\!|+1\rangle\!\rangle_y = \frac{1}{2}C_y(D_z^2 + D_z);\ |\!|0\rangle\!\rangle_y = C_y(1 - D_z^2);$$
$$|\!|-1\rangle\!\rangle_y = \frac{1}{2}C_y(D_z^2 - D_z) \quad (4)$$

where $|\!|n\rangle\!\rangle_m$ is the bra- and ket- notation of Sanctuary[48,68] ($m = x, y, z$). Evolution and relaxation of the three lines during the $^{13}C^\alpha$ CPMG [delay T (Figure 1)] due to interactions with attached α-deuterons can be described in the classical fashion:

$$\frac{d}{dt}\begin{bmatrix}|\!|+1\rangle\!\rangle_x\\ |\!|+1\rangle\!\rangle_y\\ |\!|0\rangle\!\rangle_x\\ |\!|0\rangle\!\rangle_y\\ |\!|-1\rangle\!\rangle_x\\ |\!|-1\rangle\!\rangle_y\end{bmatrix} = -\begin{bmatrix}\Gamma_1+\Gamma_2 & 2\pi J & -\Gamma_1 & 0 & -\Gamma_2 & 0\\ -2\pi J & \Gamma_1+\Gamma_2 & 0 & -\Gamma_1 & 0 & -\Gamma_2\\ -\Gamma_1 & 0 & 2\Gamma_1 & 0 & -\Gamma_1 & 0\\ 0 & -\Gamma_1 & 0 & 2\Gamma_1 & 0 & -\Gamma_1\\ -\Gamma_2 & 0 & -\Gamma_1 & 0 & \Gamma_1+\Gamma_2 & -2\pi J\\ 0 & -\Gamma_2 & 0 & -\Gamma_1 & 2\pi J & \Gamma_1+\Gamma_2\end{bmatrix}\begin{bmatrix}|\!|+1\rangle\!\rangle_x\\ |\!|+1\rangle\!\rangle_y\\ |\!|0\rangle\!\rangle_x\\ |\!|0\rangle\!\rangle_y\\ |\!|-1\rangle\!\rangle_x\\ |\!|-1\rangle\!\rangle_y\end{bmatrix} \quad (5)$$

where J is $^1J_{C^\alpha D^\alpha}$ one-bond scalar coupling and

$$\Gamma_1 = \frac{3\pi^2}{10}(QCC)^2[J(\omega_D)];\ \Gamma_2 = \frac{3\pi^2}{10}(QCC)^2[2J(2\omega_D)] \quad (6)$$

and all definitions are as in eqs 2 and 3. Each $180_y°$ Q3 pulse applied during the CPMG period interchanges the x components of the outer lines of the triplet ($|\!|+1\rangle\!\rangle_x$ and $|\!|-1\rangle\!\rangle_x$). Two experiments were recorded for each chosen CPMG duration: (a) without ^2H decoupling during CPMG period T and (*b*) with ^2H decoupling. The ratio of cross-peak intensities obtained in the two data sets (I_a/I_b) can be analyzed by numerical integration of eq 5 with the D^α QCC value as a single fitted parameter. The length of the CPMG Q3-shaped pulses is adjusted to cover the range of all aliphatic ^{13}C chemical shifts without disturbing C′ nuclei. As a result, the evolution of $^{13}C^\alpha-^{13}C^\beta$ couplings during the CPMG delay restricts the duration of total CPMG period T to multiples of $1/^1J_{C^\alpha C^\beta}$. For sensitivity reasons, only three T delays were used in this work corresponding to $k/^1J_{C^\alpha C^\beta}$ ($k = 1$, 2, or 3). Importantly, relaxation of $^{13}C^\alpha$ nuclei due to other mechanisms (e.g., $^{13}C^\alpha-D^\alpha$ dipolar, $^{13}C^\alpha$ CSA, chemical exchange) or their evolution due to scalar couplings during the CPMG period does not affect I_a/I_b ratios, as these processes contribute identically to intensities I_a and I_b.[5] Figure 3a shows a region of the 2D $^1HN-^{15}N$ correlation map of [U-^{15}N,^{13}C,^2H]-ubiquitin obtained using the HN(CACO) $^{13}C^\alpha$ CPMG experiment with a T of 84 ms ($\sim 3/^1J_{C^\alpha C^\beta}$) acquired with (top) and without (bottom) ^2H decoupling. Of note, the 2ζ delays between CPMG pulses are chosen to ensure a moderate decay of relative signal intensity without ^2H decoupling even for long T periods. The element enclosed in the dashed rectangle in Figure 1 is designed to eliminate the residual signal from protonated $^{13}C^\alpha$ positions that, if not eliminated, can artifactually increase I_a/I_b ratios because ^2H decoupling would not affect $^{13}C^\alpha$ relaxation in $^{13}C^\alpha-^1H^\alpha$ spin systems. Omission of this element in the experiments recorded on ubiquitin in this work resulted in slightly (~2.0 kHz) but uniformly lower extracted D^α QCC values.

Full treatment of the evolution of X−D spin pairs during CPMG pulse trains, which includes the effects of $^{13}C^\alpha-D^\alpha$ dipolar/D^α quadrupolar cross-correlated relaxation,[48] has been presented for the case of $^{15}N-D$ spin pairs by LiWang and Bax[5] and is adapted to $^{13}C^\alpha-D^\alpha$ spin systems in the Supporting Information. A least-squares fit using the full treatment (eqs S1−S3 of the Supporting Information) results in D^α QCC values that are on average 1.3 ± 0.2 kHz lower than those obtained using eqs 5 and 6 and the real part of the spectral density function (eq 1) confirming that the effect of dipolar/quadrupolar cross-correlations is very small and is, in fact, within the error

(66) Clore, G. M.; Szabo, A.; Bax, A.; Kay, L. E.; Driscoll, P. C.; Gronenborn, A. M. *J. Am. Chem. Soc.* **1990**, *112*, 4989–4991.
(67) Boyd, J.; Mal, T. K.; Soffe, N.; Campbell, I. D. *J. Magn. Reson.* **1997**, *124*, 61–71.
(68) Sanctuary, B. C.; Selwyn, L. *J. Chem. Phys.* **1981**, *74*, 906–912.

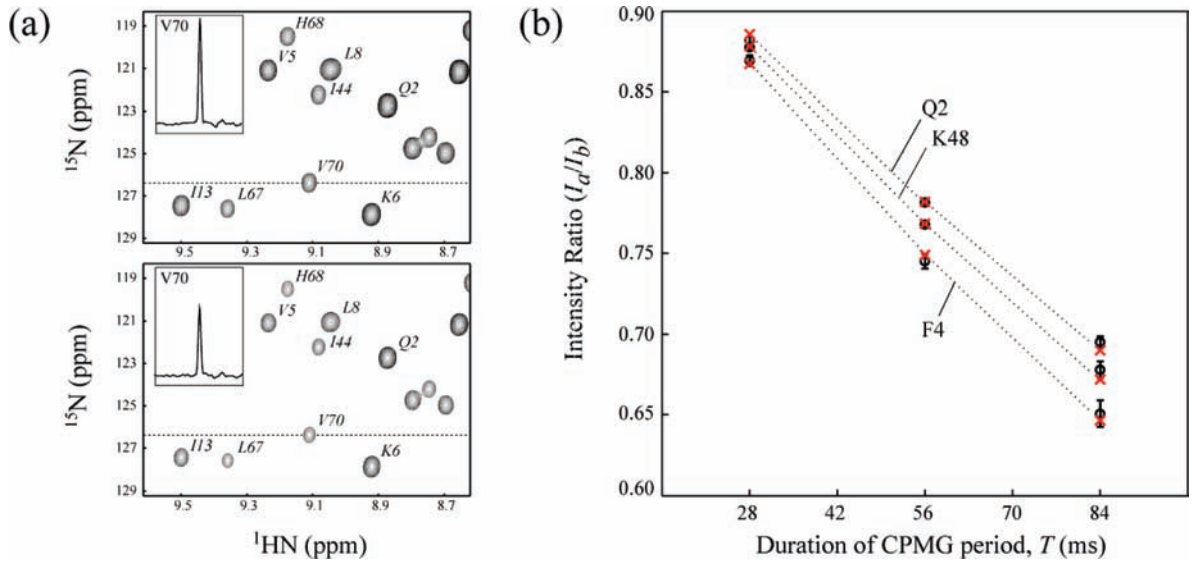

Figure 3. (a) Region of the 2D ^{1}HN−^{15}N correlation map of [U-^{15}N,^{13}C,^{2}H]-ubiquitin obtained using the HN(COCA) $^{13}C^{\alpha}$ CPMG experiment of Figure 1 ($T = 84$ ms; 27 °C; 600 MHz) with ^{2}H decoupling (top) and without ^{2}H decoupling (bottom) during the CPMG pulse train. The ratio of peak intensities in the bottom and top spectra is typically in the range from 0.64 to 0.70 for a T of 84 ms. One-dimensional slices drawn at the position of Val^{70} (shown with a dashed lines) are shown in the insets. (b) Examples of intensity ratio (I_a/I_b) decays in the $^{13}C^{\alpha}$ CPMG experiment as a function of the total CPMG duration T for Gln^{2}, Lys^{48}, and Phe^{4} of ubiquitin. Experimental ratios are shown with black open circles, while the fitted values are represented by red crosses. The extracted D^{α} QCC values are 166.2, 177.5, and 171.2 kHz for Gln^{2}, Lys^{48}, and Phe^{4}, respectively.

of extracted D^{α} QCC for most of the residues. Nevertheless, to avoid systematic overestimation of QCC values, all $^{13}C^{\alpha}$ CPMG data in this work were fit to eqs S1−S3. Examples of the I_a/I_b intensity ratio decays in the $^{13}C^{\alpha}$ CPMG experiment as a function of the total CPMG duration T for Gln^{2}, Lys^{48}, and Phe^{4} of ubiquitin are shown in Figure 3b.

Although the indirect ($^{13}C^{\alpha}$ CPMG-based) QCC determination is generally less accurate and substantially more experimentally demanding than the direct [$R^{Q}(D_{+})$,$R^{Q}(D_{z})$]-based approach described in the previous section, similar D^{α} QCC values have been obtained with the pairwise rmsd of 3.2 (3.4) kHz between the sets of QCC values obtained via scalar relaxation and [$R^{Q}(D_{+})$,$R^{Q}(D_{z})$] using $S^{2}_{C^{\alpha}-H^{\alpha}}$ from MD ($^{13}C_{\alpha}$ relaxation). The sources of disagreement between the two QCC measurements are manifold and arise from intrinsic inaccuracies of both QCC determination methods due to uncertainties in local dynamics parameters (both methods) and $^{1}J_{C^{\alpha}D^{\alpha}}$ couplings in the indirect technique. For example, the indirectly determined values of D^{α} QCC are strongly dependent upon the chosen value of $^{1}J_{C^{\alpha}D^{\alpha}}$. The exact value of this scalar coupling is difficult to measure: $^{1}J_{C^{\alpha}H^{\alpha}}$ couplings are accurately measured and subsequently scaled by the factor γ_D/γ_H. This is the best available experimental estimate of $^{1}J_{C^{\alpha}D^{\alpha}}$ (∼22 Hz) necessary for analysis of $^{13}C^{\alpha}$ CPMG experiments. Simulations show that an error in $^{1}J_{C^{\alpha}D^{\alpha}}$ as small as 0.45 Hz (∼2%) can introduce an error of ∼3.5 kHz in QCC determination, while an error of 0.02 in $S^{2}_{C^{\alpha}-H^{\alpha}}$ leads to an only ∼1.8 kHz error in QCC. It is also noteworthy that a smaller subset of D^{α} QCC values could be determined by the $^{13}C^{\alpha}$ CPMG-based approach since only 70% of the analyzed residues (whose spectral density can be reproduced with $S^{2}_{C^{\alpha}-D^{\alpha}}$ and $\tau' = 0$) gave reproducible results and at the same time passed the χ^{2} test of the fit (95% confidence threshold). It has not escaped our attention that small scalar couplings of $^{13}C^{\alpha}$ to side chain deuterons ($^{2}J_{C^{\alpha}D^{\beta}}$ and $^{3}J_{C^{\alpha}D^{\gamma}}$) may potentially compromise the $^{13}C^{\alpha}$ CPMG results. However, in this case, one would expect an overestimation of D^{α} QCC values in a significant number of residues due to additional sources of scalar relaxation. This is not consistent with the experimental data as discussed below.

Variability of D^{α} QCC Values in Ubiquitin Suggests Formation of Weak $C^{\alpha}-H^{\alpha}\cdots O{=}C$ Hydrogen Bonds. Panels a−d of Figure 4 show histograms of D^{α} QCC distributions obtained in ubiquitin using (a) R_1 and R_2 D^{α} ^{2}H rates and MD-derived $S^{2}_{C^{\alpha}-H^{\alpha}}$, (b) $^{13}C^{\alpha}$ CPMG measurements and MD-derived $S^{2}_{C^{\alpha}-H^{\alpha}}$, (c) R_1 and R_2 D^{α} ^{2}H rates and $^{13}C^{\alpha}$ relaxation-derived $S^{2}_{C^{\alpha}-H^{\alpha}}$, and (d) $^{13}C^{\alpha}$ CPMG data and $^{13}C^{\alpha}$ relaxation-derived $S^{2}_{C^{\alpha}-H^{\alpha}}$. The means of the distributions are very similar in all cases, with the largest standard deviations for the data sets obtained using the $^{13}C^{\alpha}$ CPMG-based approach. The set of residues with the lowest QCC values (shown with arrows in Figure 4) can be reproduced from one data set to another. These sites correspond to the residues whose distances from H^{α} atoms to the nearest carbonyl oxygen are less than 2.5 Å in the crystallographic structures of ubiquitin. The shortest measured $C^{\alpha}-H^{\alpha}\cdots O{=}C$ distance is between the donor−acceptor pair (Thr^{66}−Phe^{4}). Remarkably, Thr^{66} has the lowest D^{α} QCC value in two of four data sets (Figure 4b,d) and the second lowest in the data sets of Figure 4a,c, with QCC values of 164.6 ± 0.7 (Figure 4a), 161.1 ± 2.1 (Figure 4b), 162.7 ± 0.7 (Figure 4c), and 159.2 ± 2.0 (Figure 4d).

Table 1 lists the residues of ubiquitin with the shortest $C^{\alpha}-H^{\alpha}\cdots O{=}C$ distances (<2.5 Å in the X-ray structure 1ubq) and their corresponding average D^{α} QCC values (the full list of the average D^{α} QCC values is given in Table S1 of the Supporting Information). Because the X-ray structure of ubiquitin has only medium resolution (1.8 Å),[42] the uncertainties in distances and hydrogen bond lengths should be on the order of 0.1−0.2 Å. We have, therefore, extended our analysis in Table 1 to the $C^{\alpha}-H^{\alpha}\cdots O{=}C$ distances in the X-ray structure of chemically synthesized ubiquitin[69,70] (PDB entry 1ubi) and the ensemble of 10 NMR structures.[71] There are eight residues in

(69) Ramage, R.; Green, J.; Muir, T. W.; Ogunjobi, O. M.; Love, S.; Shaw, K. *Biochem. J.* **1994**, *299*, 151–158.

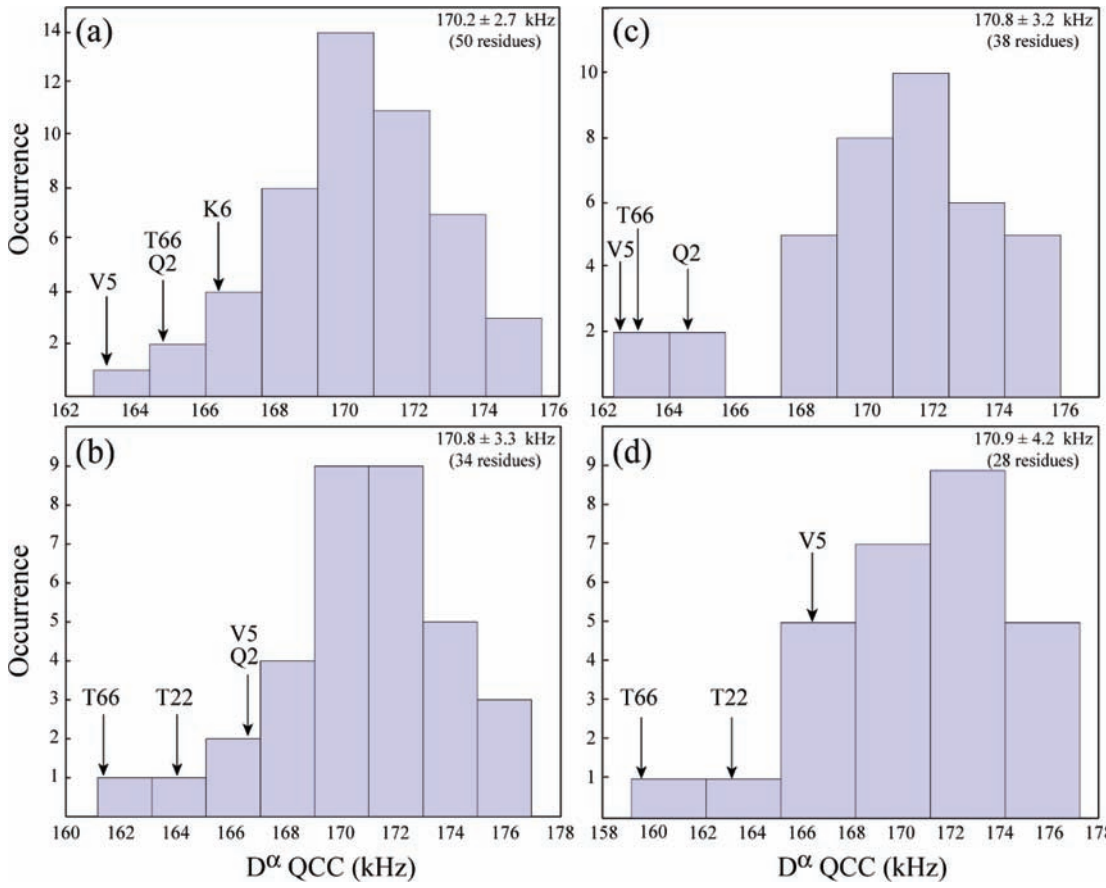

Figure 4. Histograms of D^{α} QCC values obtained in ubiquitin using (a) R_1 and R_2 D^{α} ^2H rates and $S^2_{C^{\alpha}-H^{\alpha}}$ order parameters from MD simulations, (b) $^{13}C^{\alpha}$ CPMG measurements and $S^2_{C^{\alpha}-H^{\alpha}}$ order parameters from MD simulations, (c) R_1 and R_2 D^{α} ^2H rates and $S^2_{C^{\alpha}-H^{\alpha}}$ from $^{13}C^{\alpha}$ relaxation rate measurements, and (d) $^{13}C^{\alpha}$ CPMG measurements and $S^2_{C^{\alpha}-H^{\alpha}}$ order parameters from $^{13}C^{\alpha}$ relaxation. The means and standard deviations of D^{α} QCC distributions and the total number of residues are indicated in the top right corner of each panel. Approximate positions of the residues with the lowest D^{α} QCC values in each distribution are shown with arrows.

Table 1. Residues with the Shortest $C^{\alpha}-H^{\alpha}\cdots O{=}C$ Distances in the Structures of Ubiquitin and Their Corresponding Average D^{α} QCC Values[a]

H^{α}	O	$r_{H^{\alpha}-O}$ (PDB entry 1ubq)	$r_{H^{\alpha}-O}$ (PDB entry 1ubi)	$r_{H^{\alpha}-O}$ (PDB entry 1d3z)[b]	secondary structure[c]	D^{α} QCC (kHz)[d]
Thr^{66}	Phe^{4}	2.22	2.27	2.32−2.35	β5	162.0 ± 2.5
Leu^{71}	Gln^{40}	2.27	2.36	*2.53−2.72*	β5	−[f]
Thr^{55}	Asp^{21}	2.28	2.36	*2.54−2.69*	bridge	170.6 ± 2.4
Thr^{22}	Arg^{54}	2.35	2.46	2.14−*2.51*[e]	bridge	166.1 ± 3.5
Ile^{44}	Lys^{48}	2.39	2.31	2.34−*2.54*	β3	170.9 ± 3.2
Gln^{2}	Leu^{15}	2.42	2.34	2.33−2.37	β1	164.5 ± 2.0
Leu^{43}	His^{68}	2.46	2.40	2.39−*2.61*	β3	−[f]
Val^{5}	Leu^{67}	2.49	*2.55*	2.29−2.39	β1	164.9 ± 2.2

[a] Distances are calculated from the protonated crystallographic structure of ubiquitin (PDB entry 1ubq[42]), the crystal structure of the chemically synthesized ubiquitin (PDB entry 1ubi[69,70]), and the ensemble of 10 NMR structures (PDB entry 1d3z[71]). Reported are only the distances shorter than 2.5 Å in the original crystal structure (1ubq). Distances exceeding the 2.5 Å limit in other structures are italicized. [b] Reported is the range of distances observed in all the structures of the NMR ensemble. [c] The numerals in the designation of the secondary structure relate to the number of the strand in the single β-sheet of ubiquitin. The strand numbers are indicated for the donor residues. The secondary structure elements are reported as identified by Molmol.[78] [d] D^{α} QCC values obtained in the four data sets of Figure 4 are averaged. The errors reported reflect the standard deviation of the distribution obtained for each of the QCC values from the four different data sets. [e] The range of distances obtained from the "dynamically averaged" ensemble of ubiquitin structures[79] (PDB entry 1xqq) as this distance is greater than 3 Å in all NMR structures (1d3z). [f] D^{α} QCC values are not available for Leu^{71} or Leu^{43}.

the X-ray structure of ubiquitin (PDB entry 1ubq) with $C^{\alpha}-H^{\alpha}\cdots O{=}C$ distances between residues i and j ($|i-j|>1$) of <2.5 Å (Table 1); four of these eight residues consistently have significantly lower than average D^{α} QCC values (as well as the lowest QCC in the histograms of Figure 4): Thr^{66}, Gln^{2}, Val^{5}, and Thr^{22}. The assignment of Thr^{22} to this group is tentative because of the poor reproducibility of its QCC among different data sets. Although a pair of other residues (notably, Lys^{29} and Lys^{6}) have low QCC values in at least one of the data sets in Figure 4 but $C^{\alpha}-H^{\alpha}\cdots O{=}C$ distances exceeding 2.5 Å in the crystal structure of ubiquitin, the observed correspondence between short $C^{\alpha}-H^{\alpha}\cdots O{=}C$ distances and

(70) Alexeev, D.; Bury, S. M.; Turner, M. A.; Ogunjobi, O. M.; Muir, T. W.; Ramage, R.; Sawyer, L. *Biochem. J.* **1994**, *299*, 159–163.

(71) Cornilescu, G.; Marquardt, J.; Ottiger, M.; Bax, A. *J. Am. Chem. Soc.* **1998**, *120*, 6836–6837.

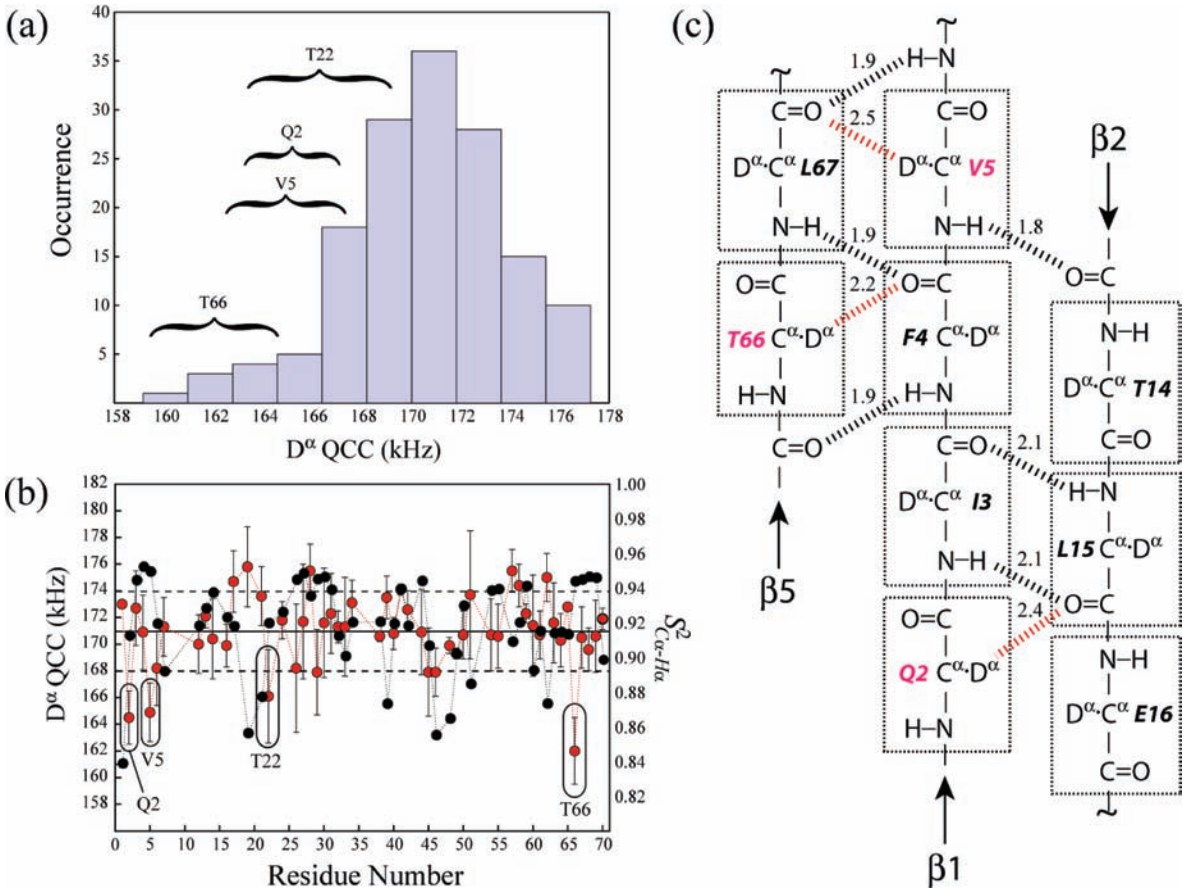

Figure 5. (a) Histogram of the combined data set of D^{α} QCC values in ubiquitin. The ranges of D^{α} QCC values of the residues likely involved in $C^{\alpha}-H^{\alpha}\cdots O{=}C$ hydrogen bonds obtained in the four data sets of Figure 4 are indicated. (b) Average D^{α} QCC values (red circles, left axis) and $S^2_{C^{\alpha}-H^{\alpha}}$ order parameters derived from MD simulations (black circles, right axis) plotted vs residue number. The mean value of D^{α} QCC is shown with a horizontal solid line, while dashed lines indicate the boundaries of the standard deviation from the mean. Error bars correspond to one standard deviation of the distribution obtained for each of the QCC values from the four data sets of Figure 4. Highlighted are the residues with the lowest D^{α} QCC values. (c) Topology diagram showing the hydrogen bonding interactions among strands $\beta1$, $\beta2$, and $\beta5$ in the β-sheet of ubiquitin. $N-H\cdots O{=}C$ hydrogen bonds and the putative $C^{\alpha}-H^{\alpha}\cdots O{=}C$ hydrogen bonds are shown with black and red dashed lines, respectively. Distances between the donors (D^{α}) and acceptor oxygens (angstroms) as measured in the X-ray structure of ubiquitin (PDB entry 1ubq) are indicated above each bond.

low QCC values strongly suggests the existence of weak hydrogen bonding interactions in which $C^{\alpha}-H^{\alpha}$ groups serve as donors and carbonyl oxygens as acceptors.

Formation of weak $C^{\alpha}-H^{\alpha}\cdots O{=}C$ hydrogen bonds[17,18,72] was recognized some time ago as a common structural motif in proteins.[73,74] $C^{\alpha}-H^{\alpha}\cdots O{=}C$ hydrogen bonds are predicted to be approximately half as strong as the much more common $N-H\cdots O{=}C$ interactions (ΔH at 25 °C of approximately −3 kcal/mol according to ab initio calculations for $H_{\alpha}\cdots O$ distances of ∼2.2−2.5 Å[75]). Ultra-high resolution protein crystal structures show that $C^{\alpha}-H^{\alpha}\cdots O{=}C$ hydrogen bonds may be accompanied by the distorted geometry of the $C^{\alpha}-H^{\alpha}$ bond with H^{α} positions bent by up to 0.3 Å toward the carbonyl oxygen.[76]

Experimental observation of $C^{\alpha}-H^{\alpha}\cdots O{=}C$ hydrogen bonds by NMR is associated with considerable difficulties. To the best of our knowledge, the first and only such observation by solution NMR has been reported by Grzesiek and co-workers via the measurement of small inter-residue (trans-hydrogen bond) $^{h3}J_{C^{\alpha}C'}$ scalar couplings (∼0.3 Hz) in protein G.[19] In our hands, after the 4 day long acquisition, the long-range H(NCO)CA experiment[19] performed with the 3 mM sample of [U-^{15}N,^{13}C,^{2}H]-ubiquitin did not provide any trans-hydrogen bond $^{13}C'-^{13}C^{\alpha}$ correlations that could be identified with confidence. Therefore, in this work, we have to rely on the analysis of $C^{\alpha}-H^{\alpha}\cdots O{=}C$ distances in the X-ray and solution structures of ubiquitin in relationship to the measured D^{α} QCC values.

Typically, an ultra-high resolution (<1 Å) crystal structure of a protein is needed to draw definitive conclusions about the existence of these weak interactions.[76,77] Overlap of electronic wave functions of the donor and acceptor groups in a hydrogen bond may increase the symmetry of the electronic environment, leading to smaller electric field gradients at the nucleus and a concomitant decrease in QCC values. D^{α} QCC can therefore potentially serve as a sensitive probe for identification of weak $C^{\alpha}-H^{\alpha}\cdots O{=}C$ hydrogen bonding interactions in proteins.

As the distributions in Figure 4 do not provide insight into the variability of individual D^{α} QCC values between different data sets, Figure 5a shows a histogram of the combined data

(72) Steiner, T. *Chem. Commun.* **1997**, 727–734.
(73) Derewenda, Z. S.; Lee, L.; Derewenda, U. *J. Mol. Biol.* **1995**, *252*, 248–62.
(74) Wahl, M. C.; Sundaralingham, M. *Trends Biochem. Sci.* **1997**, *22*, 97–102.
(75) Vargas, R.; Garza, J.; Dixon, D. A.; Hay, B. P. *J. Am. Chem. Soc.* **2000**, *122*, 4750–4755.
(76) Addlagatta, A.; Krzywda, S.; Czapinska, H.; Otlewski, J.; Jaskolski, M. *Acta Crystallogr.* **2001**, *D57*, 649–663.
(77) Esposito, L.; Vitagliano, L.; Sica, F.; Sorrentino, G.; Zagari, A.; Mazzarella, L. *J. Mol. Biol.* **2000**, *297*, 713–732.

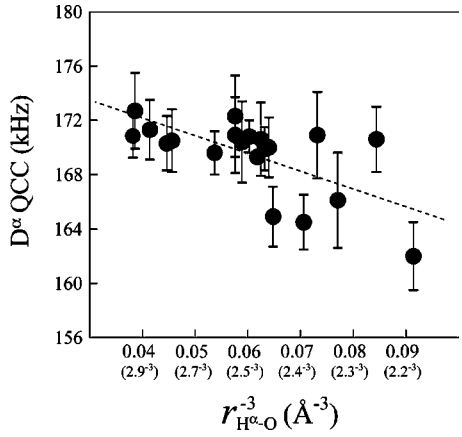

Figure 6. Linear correlation plot of D^{α} QCC values (*y*-axis) vs the inverse cube of $H^{\alpha}\cdots O$ distances (*x*-axis, $Å^{-3}$) in ubiquitin (PDB entry 1ubq). The cutoff value of 3 Å was used in the calculation of $C^{\alpha}-H^{\alpha}\cdots O{=}C$ distances. The Pearson $R = -0.64$ (19 residues). The dashed curve corresponds to the linear regression fit with *y* being equal to $177.4 \pm 2.4 - 130.6 \pm 38.3x$. D^{α} QCC values obtained in the four data sets of Figure 4 are averaged. Error bars correspond to one standard deviation of the distribution obtained for each of the QCC values from the four data sets.

set that indicates the ranges of D^{α} QCC values for the residues that are likely to be involved in $C^{\alpha}-H^{\alpha}\cdots O{=}C$ hydrogen bonds. The D^{α} QCC values averaged over all the data sets of Figure 4 are plotted as a function of residue number in Figure 5b together with the MD-derived $S^2_{C^{\alpha}-H^{\alpha}}$ order parameters. The average value of D^{α} QCC in the combined data set is 170.6 ± 3 kHz, indicating that the uniform D^{α} QCC of 174 kHz adopted in our previous ^2H relaxation study[15] is closer to the upper bound of possible QCC values. The distribution of the combined set is slightly skewed (similar to distributions of individual sets in Figure 4) with a small number of residues likely involved in $C^{\alpha}-H^{\alpha}\cdots O{=}C$ hydrogen bonds having significantly lower QCC values (Figure 5a and Table 1).

The $C^{\alpha}-H^{\alpha}\cdots O{=}C$ hydrogen bonds in proteins are commonly observed in β-sheets and are more rare in α-helices.[73,80] Three of four residues highlighted in panels a and b of Figure 5 (Thr^{66}, Gln^2, and Val^5) are located in strands 1 and 5 of the β-sheet, while Thr^{22} is located in a turn (Table 1). Figure 5c shows the topology diagram of hydrogen bonding interactions among strands $\beta1$, $\beta2$, and $\beta5$ in ubiquitin. In agreement with earlier observations,[19,73,75] all $C^{\alpha}-H^{\alpha}\cdots O{=}C$ hydrogen bonds in Figure 5c have a bifurcated topology with one of the free electron pairs of acceptor oxygens forming a $N-H\cdots O$ bond while the other electron pair of the same oxygen is involved in a $C^{\alpha}-H^{\alpha}\cdots O{=}C$ interaction. Interestingly, in the crystal structure of ubiquitin, the amides of Gln^2, Thr^{66}, and Thr^{22} are not hydrogen-bonded to either backbone, side chain, or water oxygens. Furthermore, the amides of residues preceding Gln^2 and Thr^{66} (Met^1 and Ser^{65}) are also devoid of hydrogen bonds. Formation of weak $C^{\alpha}-H^{\alpha}\cdots O{=}C$ hydrogen bonds with the participation of Gln^2, Thr^{66}, and Thr^{22} might provide (partial) enthalpic compensation for the lack of amide hydrogen bonding in these regions of ubiquitin structure.

Figure 6 shows a correlation plot of D^{α} QCC values versus the inverse cube of short (<3 Å) $C^{\alpha}-H^{\alpha}\cdots O{=}C$ distances ($r^{-3}_{H^{\alpha}-O}$) in ubiquitin (PDB entry 1ubq). The anticorrelation is moderate (Pearson's $R = -0.64$ for 19 observations) but statistically significant, with the probability of exceeding *R* in a random set of data being <0.5%.[49] Linear regression analysis of the data in Figure 6 yields the following relationship between QCC (in kHz) and $r^{-3}_{H^{\alpha}-O}$ (in $Å^{-3}$): $QCC = 177.4 - 130.6\ r^{-3}_{H^{\alpha}-O}$. The inclusion of angular terms accounting for the nonlinearity of $C^{\alpha}-H^{\alpha}\cdots O{=}C$ hydrogen bonds does not lead to the improvement of this correlation. Alternative distance parametrizations are possible. For example, QCC versus $a\exp(-br_{H^{\alpha}-O}) + c$ yields the following: $a = -43696$, $b = 3.9$, $c = 171.95$, and a correlation coefficient of -0.65. The small number of low D^{α} QCC values that correspond to short $C^{\alpha}-H^{\alpha}\cdots O{=}C$ distances and the uncertainties in the distances in the medium-resolution X-ray structures of ubiquitin preclude more accurate empirical parametrization of D^{α} QCC versus the distances and angles of $C^{\alpha}-H^{\alpha}\cdots O{=}C$ hydrogen bonds. Nevertheless, the correlation in Figure 6 implies that weak $C^{\alpha}-H^{\alpha}\cdots O{=}C$ hydrogen bonding is likely to be the primary source of variability of D^{α} QCC values in proteins. Additional variations in D^{α} QCC may arise from close contacts with other oxygen acceptors in protein structures (Thr and Ser O^{γ} and Asp/Glu $O^{\delta/\varepsilon}$ positions) as well as water oxygens and possibly nitrogen acceptors. No attempt to account for these interactions has been undertaken here. We note that the derived D^{α} QCC values show no quantitative relationship to ϕ or ψ backbone dihedral angles of ubiquitin structure (Figure S1 of the Supporting Information).

The range of D^{α} QCC values in Figure 5 is in good agreement with previous solid-state NMR measurements. Several solid-state NMR studies have reported the values of QCC for aliphatic deuterons attached to sp^3-hybridized carbons ranging from 168 ± 2 to 174 ± 2 kHz.[81] In the context of this study, of special interest are the solid-state NMR measurements of Haeberlen and co-workers that provided substantially different QCC values for the two α-deuterons in zwitterionic glycine: 159.9 and 169.4 kHz.[6] The authors ascribe the large difference between the two values to formation of weak $C^{\alpha}-H^{\alpha}\cdots O$ hydrogen bonds with oxygen acceptors located in an adjacent layer of glycine molecules leading to a decrease in the QCC in one of the two α-deuterons.[6] What is determined in single-crystal NMR measurements is the product $\sqrt{S^2} \times$ QCC, where S^2 is the squared order parameter of local motions which are assumed to be axially symmetric. If S^2 is assumed to be equal to 0.95,[5,62] then the measurements of Haeberlen and co-workers in α-glycine yield a QCC value of 173.8 kHz for the non-hydrogen-bonded α-deuteron and 164.1 kHz for the hydrogen-bonded one.

Concluding Remarks

In summary, we have shown that quadrupolar coupling constants of α-deuterons in ubiquitin can be measured by solution NMR spectroscopy with an accuracy sufficient for predicting the location of weak $C^{\alpha}-H^{\alpha}\cdots O{=}C$ hydrogen bonds. Quadrupole coupling constants of α-deuterons are sensitive to the local electronic environment at the nucleus and may serve as useful probes of $C^{\alpha}-H^{\alpha}\cdots O{=}C$ hydrogen bonding in proteins. The average D^{α} QCC value of 171 ± 3 kHz has been derived from the averaged set of couplings. The variability and the mean of D^{α} QCC values in ubiquitin are significantly lower than those of amide deuterons ($\sim 215 \pm 9$ kHz),[2,5] where hydrogen-bonding effects are more pronounced due to much

(78) Koradi, R.; Billeter, M.; Wüthrich, K. *J. Mol. Graphics* **1996**, *14*, 51–55.
(79) Lindorff-Larsen, K.; Best, R. B.; Depristo, M. A.; Dobson, C. M.; Vendruscolo, M. *Nature* **2005**, *433*, 128–132.
(80) Bella, J.; Berman, H. M. *J. Mol. Biol.* **1996**, *264*, 734–742.
(81) Burnett, L. H.; Muller, B. H. *J. Chem. Phys.* **1971**, *55*, 5829–5831.

shorter hydrogen bond lengths (Figure 5c). On the other hand, the D^{α} QCC values are substantially higher on average and more variable than the QCC values of methyl deuterons in proteins (167 ± 1 kHz)[16] that are unlikely to participate in the formation of $H^{m}\cdots O$ hydrogen bonds because of fast rotation about the methyl 3-fold axis. A statistically significant anticorrelation of D^{α} QCC with the inverse cube of short $C^{\alpha}-H^{\alpha}\cdots O{=}C$ distances in ubiquitin has been established.

Extremely high resolution X-ray or neutron diffraction protein structures are required to infer the existence of $C^{\alpha}-H^{\alpha}\cdots O{=}C$ hydrogen bonds in proteins. On the other hand, as we show in this work, a substantial body of high-quality NMR data needs to be accumulated to unambiguously establish the presence of these weak interactions in solution via D^{α} QCC measurements. This presently restricts the applicability of the described methodology for QCC determination to a relatively small subset of "well-behaved" proteins that provide spectra with high signal-to-noise ratios and, as a result, can be very well characterized by a plethora of solution NMR techniques. Nevertheless, this study demonstrates how the combined use of D^{α} quadrupolar coupling constants and dynamics information permits the identification of weak hydrogen bonding effects in proteins that may be difficult or impossible to detect by other means.

Acknowledgment. This work was supported in part by a National Science Foundation grant to R.B. (MCB-0918362). V.T. thanks the University of Maryland for continuous support. We thank Dr. Chenyun Guo (University of Maryland) for providing the [2-$^{13}C_1$]-glucose-derived and ^{15}N- and ^{13}C-labeled samples of ubiquitin and Dr. Byrd (National Cancer Institute, Frederick, MD) for the generous gift of the [U-^{15}N,^{13}C,^{2}H]-ubiquitin.

Supporting Information Available: $^{13}C^{\alpha}$ relaxation-derived $S^2_{C^{\alpha}-H^{\alpha}}$ order parameters, $S^2_{C^{\alpha}-D^{\alpha}}$ order parameters derived from ^{2}H D^{α} rates, MD-derived $S^2_{C^{\alpha}-H^{\alpha}}$ order parameters, and average D^{α} QCC values in ubiquitin (Table S1), plots of D^{α} QCC values versus backbone dihedral angles (ϕ and ψ) of ubiquitin (Figure S1), and a brief theoretical description of the evolution of a $^{13}C^{\alpha}-D^{\alpha}$ spin system during CPMG pulse trains. This material is available free of charge via the Internet at http://pubs.acs.org.

JA101691S